

The Usefulness of Virtual Fluoroscopic Preprocedural Planning During Percutaneous Transhepatic Biliary Drainage

Mitsuhiro Kinoshita¹ · Ryozo Shirono² · Katsuya Takechi² · Hironobu Yonekura³ · Seiji Iwamoto⁴ · Takayoshi Shinya¹ · Shoichiro Takao⁵ · Masafumi Harada⁴

Received: 27 October 2016 / Accepted: 17 January 2017

© Springer Science+Business Media New York and the Cardiovascular and Interventional Radiological Society of Europe (CIRSE) 2017

Abstract

Purpose To retrospectively evaluate the usefulness of virtual fluoroscopic preprocedural planning (VFPP) in the percutaneous transhepatic biliary drainage (PTBD) procedure.

Materials and Methods Twenty-two patients who were treated by PTBD were included in this study. Twelve patients were treated using PTBD intraoperative referencing coronal computed tomography (CT) images (i.e., coronal CT group), and ten patients were treated using PTBD intraoperative referencing VFPP images (i.e., VFPP group). To analyze the effect of the intraoperative referencing VFPP image, the VFPP group was retrospectively compared with the coronal CT group.

Results The characteristics of both patient groups were not statistically significantly different. There were no

significant differences in the targeted bile duct, diameter and depth of the target bile, breath-holding ability, number of targeted bile duct puncture attempts, change in the targeted bile duct, and exchange of the drainage catheter. However, the X-ray fluoroscopy time and the procedure time were significantly shorter in the VFPP group than in the coronal CT group (196 vs. 334 s, $P < 0.05$; and 16.0 vs. 27.2 min, $P < 0.05$).

Conclusion Intraoperative referencing using the VFPP imaging in PTBD intuitively can be a useful tool for better localization of the guidewire in the bile duct and thereby shorten the X-ray fluoroscopy time and procedure time while minimizing radiation exposure and complications.

Keywords Virtual fluoroscopic preprocedural planning · Virtual fluoroscopy · Percutaneous transhepatic biliary drainage · Procedure time · Ray Summation image · X-ray fluoroscopy time

✉ Mitsuhiro Kinoshita
kinoshita.3216@tokushima-u.ac.jp

¹ Department of Radiology (Diagnostic Radiology), Tokushima University Hospital, 2-50-1, Kuramoto-cho, Tokushima City, Tokushima 770-8503, Japan

² Department of Radiology, Tokushima Red Cross Hospital, 103 Irinokuchi Komatsushima-cho, Komatsushima City, Tokushima 773-8502, Japan

³ Department of Radiological Technology, Tokushima Red Cross Hospital, 103 Irinokuchi Komatsushima-cho, Komatsushima City, Tokushima 773-8502, Japan

⁴ Department of Radiology and Radiation Oncology, Institute of Biomedical Sciences, Tokushima University Graduate School, 3-18-15, Kuramoto-cho, Tokushima City, Tokushima 770-8509, Japan

⁵ Department of Diagnostic Radiology, Tokushima University Graduate School of Health Science, 3-18-15, Kuramoto-cho, Tokushima City, Tokushima 770-8509, Japan

Introduction

Percutaneous transhepatic biliary drainage (PTBD) is an established interventional procedure for treating patients with malignant or benign biliary obstruction [1–7]. A recent quality improvement guideline for PTBD reported that the threshold of success rate for dilated ducts is 95% [5]. However, PTBD is an invasive technique and has some associated complications [6]. The recommended overall procedure threshold for all major complications of PTBD is 10% [5]. Complications can be categorized as “early” (i.e., occurring within 30 days) or “late.” Approximately one-half of early complications are procedure-related [8–10]. Thus, it is important that the procedure is performed precisely and quickly to reduce complications.

We have used virtual fluoroscopic preprocedural planning (VFPP) as a new navigation system to perform PTBD precisely and quickly. Virtual fluoroscopic preprocedural planning involves using an image in which trace lines are drawn along ductal structures (e.g., vessels or the biliary duct) on a Ray Summation image, which is similar to a fluoroscopy image, and it is easy to prepare using volume data from multiple-detector computed tomography (MDCT) and workstation [11]. Fukusumi et al. [11] reported the feasibility of VFPP in bronchoscopy. However, to our knowledge, there has yet been no report on the usefulness of VFPP in the PTBD procedure. Therefore, the purpose of this study was to retrospectively evaluate the usefulness of VFPP in the PTBD procedure.

Materials and Methods

Patients

Between April 2014 and 2016 in the Department of Radiology at a single hospital, first-attempt PTBD was performed in 24 consecutive patients with obstructive jaundice due to biliary obstruction. We excluded two patients because the first-attempt PTBD was unsuccessful on account of the small caliber of the target duct. Thus, 22 patients (11 men and 11 women; mean age 76.8 years; range 62–91 years) were included in this study. The causes of malignant biliary obstruction were pancreatic cancer ($n = 7$), cholangiocarcinoma ($n = 3$), lymph node metastasis of gastric cancer ($n = 3$), recurrent gastric cancer ($n = 2$), carcinoma of the ampulla of Vater ($n = 1$), gallbladder cancer ($n = 1$), and right renal pelvic cancer ($n = 1$). The cause of benign biliary obstruction was choledocholithiasis ($n = 4$). Twelve patients were treated by PTBD using intraoperative referencing coronal computed tomography (CT) images (i.e., coronal CT group), and ten patients were treated by PTBD using intraoperative VFPP images (i.e., VFPP group). The institutional review board approved this retrospective study, and no individual patient consent was required. All patients were informed about the benefits and potential risks of the procedure. All patients provided written informed consent.

The PTBD Procedure

All procedures were performed by two interventional radiologists with at least 10 years of experience with interventional techniques in the angiography suite. All patients were initially scanned by ultrasound (US) using a 3.5-MHz electronic convex probe (F37; Hitachi, Tokyo, Japan), and a CT scan was performed using the Somatom

Sensation Cardiac 64 scanner (Siemens Medical Solutions, Forchheim, Germany). The PTBD procedures were administered in standard fashion, as described elsewhere [2, 3, 10].

After administering local anesthesia with 1% lidocaine (Xylocaine Injection; AstraZeneca, Osaka, Japan) and intravenous sedation with pentazocine hydrochloride (Sosegon Injection; Maruishi Pharmaceutical, Osaka, Japan), a 18-gauge needle (Create Medic, Kanagawa, Japan) was inserted under US guidance using a 3.5-MHz intraoperative electronic convex probe (F37; Hitachi, Tokyo, Japan) with a puncture adapter. Once the backflow of bile occurred and on successfully placing the needle tip in the bile duct, a 0.035-inch guidewire (Radifocus; Terumo, Tokyo, Japan) was advanced into the proximal obstruction under X-ray fluoroscopy guidance while using the reference coronal CT images or VFPP images. After removing the needle, a 7-French dilator (Cook Japan, Tokyo, Japan) and 7.2-French pigtail drainage catheter (Cook Japan, Tokyo, Japan) were inserted in order under X-ray fluoroscopy guidance. After placing the drainage catheter, a small amount of dilute contrast media was infused through the catheter to confirm that the catheter was in the appropriate position. If puncturing the targeted bile duct proved difficult, despite several attempts, then the other duct was punctured, and the change in protocol was recorded. If a guidewire could be advanced beyond the obstruction of the common bile duct, a 7.2-French pigtail drainage catheter, which was customized by adding side holes at the appropriate position (internal–external catheter), was placed into the small bowel.

Coronal CT Imaging

For all patients, MDCT was performed by using a Somatom Sensation Cardiac 64 scanner. The range of CT covered the area of the abdomen. The scan and reconstruction parameters of CT were 64×0.6 mm beam collimation, 120 kV X-ray tube voltage, 250 reference mAs of the X-ray tube current, and automatic exposure control (CARE Dose 4D; Siemens Medical Systems, Forchheim, Germany), 0.5-s gantry rotation time, pitch factor of 1.1, 3.0 mm slice thickness, and reconstruction intervals of 3.0 mm. The convolution kernel was B31f medium smooth+.

For the protocol with contrast material (CM), 600-mg iodine per kilogram body weight was injected for 30 s [$20 \text{ (mg kg}^{-1}\text{)/s}$ fractional dose] and the CT scan delay times were 45 and 120 s. The CM was iopamidol 300 or iopamidol 370 (Iopamiron with 300 or 370 mg of iodine per milliliter; Bayer Pharma, Osaka, Japan), depending on the patient's weight. It was injected into the brachial vein with a 22-gauge needle at a rate of 2.1–3.2 mL/s using an

automated injector (Dual Shot; Nemoto Kyorindo, Tokyo, Japan).

Contrast-enhanced MDCT was performed to all patients with a malignant biliary obstruction ($n = 18$). However, plain MDCT was performed to all patients with a benign biliary obstruction ($n = 4$).

Virtual Fluoroscopic Preprocedural Planning

Since April 2015, we have used VFPP as a new navigation system. Virtual fluoroscopic preprocedural planning uses an image that is created from the volume data obtained from MDCT imaging with a workstation; the trace lines of the bile duct or vessels on the Ray Summation image are similar to those of a fluoroscopy image [6]. Multidetector CT images of 1.0 mm thickness were transferred to a 3-dimensional workstation (SynapseVincent; Fujifilm Co., Tokyo, Japan). By referring to multiplanar reconstruction

CT images, we drew a trace line between the targeted bile duct and the common bile duct before it enters the duodenum at the major duodenal papilla along the center of the bile duct. In addition, if necessary, we drew trace lines along neighboring bile ducts and added annotations at the obstruction and the major duodenal papilla. The lines could be displayed at any angle with 3-dimensional virtual fluoroscopic image. We reconstructed the background by using a Ray Summation image, and applied an edge filter (Fig. 1). Customization of using workstation made it possible to create this image in approximately 10 min. All VFPPs were performed by two authors and included a radiologist and radiological technician. In instances of disagreement, a final consensus was reached through interobserver discussion. We applied VFPP to the PTBD procedure. Virtual fluoroscopic preprocedural planning was used as a reference to select the bile duct during the PTBD procedure.

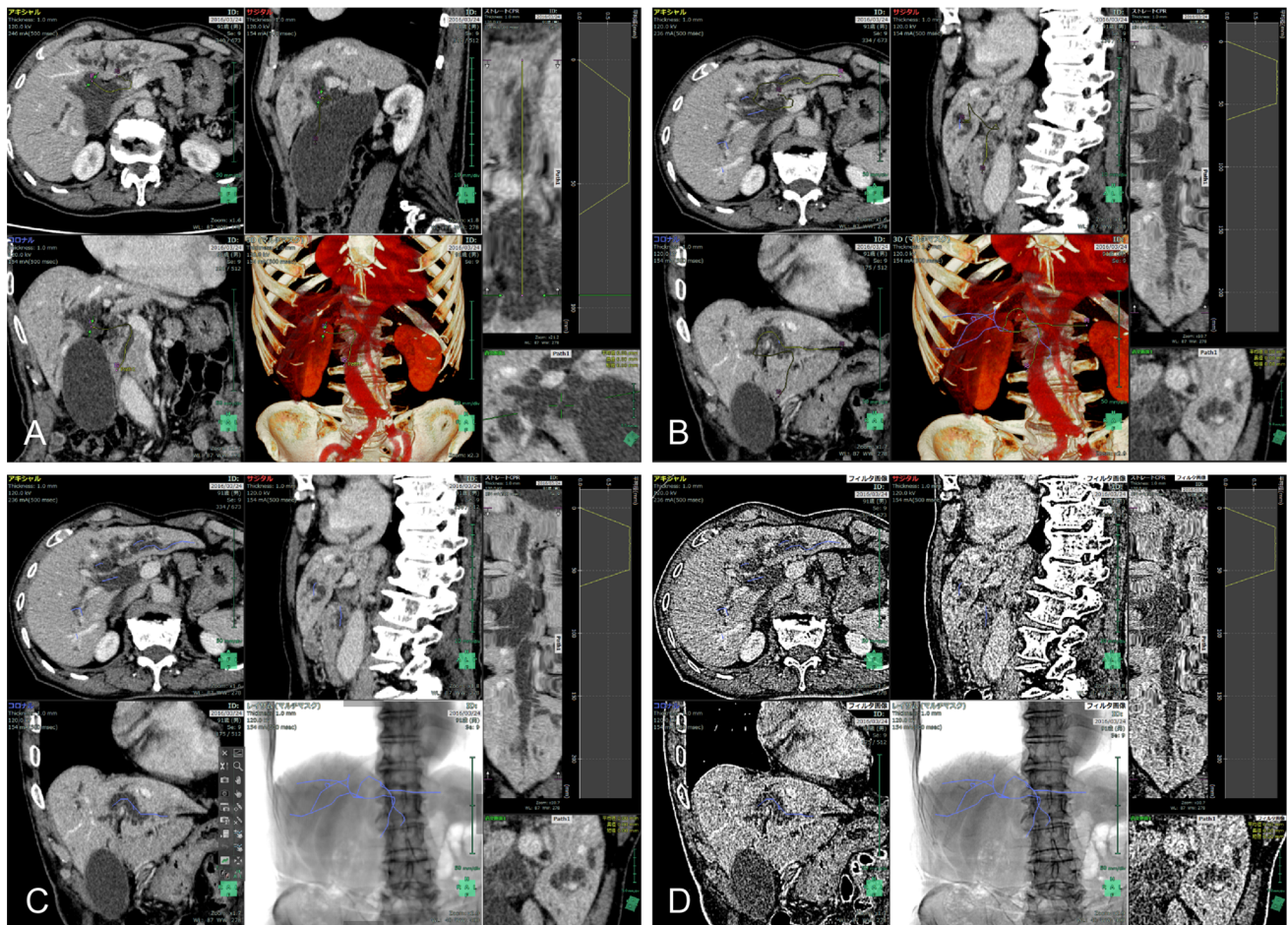


Fig. 1 The process of VFPP using a workstation. **A, B** While referencing the multiplanar reconstruction computed tomography images, we drew a trace line between the targeted bile duct, neighboring bile ducts, and common bile duct before it enters the

duodenum at the major duodenal papilla along the center of the bile duct. **C** The background is a reconstructed Ray Summation image. **D** An edge filter is applied to the background VFPP

Assessment

To analyze the effect of the intraoperative referencing VFPP image, ten consecutive patients who had undergone first-attempt PTBD using VFPP (i.e., VFPP group) were retrospectively compared with 12 consecutive patients who had undergone first-attempt PTBD using coronal CT images (i.e., coronal CT group). The Fisher's exact test or Mann–Whitney *U* test was used to evaluate significant differences in the patients' characteristics and results of the PTBD procedure in the coronal CT and VFPP groups. Categorical variables are expressed as the number and compared by Fisher's exact test. Continuous variables are expressed as the mean \pm the standard deviation and compared by the Mann–Whitney *U* test. The patients' characteristics that were examined were age, sex, body weight, etiology (i.e., benign or malignant biliary obstruction), location of the obstructing lesion (i.e., upper or lower), ascites, liver toxicity, inflammation, and jaundice. We classified the location of the obstructing lesion into two categories, based on the intraoperative cholangiopancreatography findings: (1) the "upper" location indicated that the obstructing lesion was above the point of the communication of the three ducts (i.e., cystic, common hepatic, and common bile duct), and (2) the "lower" location indicated that the obstructing lesion was below the point of the communication of the three ducts. Liver toxicity was evaluated by the aspartate aminotransferase (AST) and alanine aminotransferase (ALT) levels; inflammation was evaluated by white blood cell counts and C-reactive protein levels; and jaundice was evaluated by the serum total bilirubin level by laboratory tests that were performed within 2 days before the PTBD procedure. Percutaneous transhepatic biliary drainage involved the targeted bile

duct, diameter of the bile duct, depth of the bile duct, breath-holding ability (i.e., good or poor), number of targeted bile duct puncture attempts, change in the targeted bile duct, exchange of the drainage catheter, X-ray fluoroscopy time, and procedure time. We classified breath-holding into two grades, according to our instructions: (1) "good" was defined as breath-holding for more than 3 s, and (2) "poor" was defined as breath-holding for less than 3 s. We defined the procedure time as the time from the administration of the local anesthesia until confirming, using the contrasting media, that the catheter was in the appropriate position. Statistical significance was based on 2-sided design-based tests evaluated at $\alpha = 0.05$. All statistical analyses were performed using SPSS, version 23 (IBM, Armonk, NY, USA).

Results

The Patients' Characteristics

The characteristics of both patient groups are presented in Table 1. There were no statistically significant differences between the groups.

Results of the PTBD Procedure

The results of PTBD procedure of both groups are presented in Table 2. The targeted bile duct was B3 or B8. In the coronal CT group, B3 was targeted in eight patients and B8 was targeted in four patients. In the VFPP group, B3 was targeted in nine patients and B8 was targeted in one patient. There were no statistically significant differences between the groups.

Table 1 The patients' characteristics

	Coronal CT group ($n = 12$)	VFPP group ($n = 10$)	<i>P</i> value
Age (year)	74.6 \pm 7.29	79.4 \pm 9.67	0.159
Sex (male/female)	8/4	3/7	0.198
Body weight (kg)	43.5 \pm 11.8	48.2 \pm 7.08	0.123
Etiology (benign/malignant)	3/9	1/9	0.594
Location of the obstructing lesion (upper/lower)	0/12	2/8	0.195
Ascites (+/–)	4/8	2/8	0.646
Preoperative TB (mg/dL)	5.3 \pm 3.4	6.2 \pm 5.0	0.628
Preoperative AST (U/L)	165 \pm 103	172 \pm 106	0.872
Preoperative ALT (U/L)	146 \pm 121	169 \pm 136	0.722
Preoperative WBC (/ μ L)	9778 \pm 6289	10180 \pm 8809	0.872
Preoperative CRP (mg/dL)	7.00 \pm 8.30	6.41 \pm 6.50	0.923

ALT alanine aminotransferase, AST aspartate aminotransferase, CRP C-reactive protein, CT computed tomography, PTBD percutaneous transhepatic biliary drainage, TB total bilirubin, VFPP virtual fluoroscopic preprocedural planning, WBC white blood cell count

Table 2 Results of the PTBD procedure

	Coronal CT group ($n = 12$)	VFPP group ($n = 10$)	<i>P</i> value
Targeted bile duct (B3/B8)	8/4	9/1	0.323
Diameter of the bile duct (mm)	7.1 ± 2.8	7.2 ± 2.7	0.872
Depth of the bile duct (mm)	40.9 ± 12.1	31.9 ± 11.0	0.228
Breath-holding ability (good/poor)	11/1	9/1	1.000
Number of targeted puncture attempts (time)	1.7 ± 1.0	1.4 ± 1.0	0.456
Change in the targeted bile duct (yes/no)	2/10	1/9	1.000
Exchange of the drainage catheter (yes/no)	1/11	1/9	1.000
X-ray fluoroscopy time (s)	334 ± 231	196 ± 137	0.043*
Procedure time (min)	27.2 ± 13.9	16.0 ± 9.65	0.021*

CT computed tomography, PTBD percutaneous transhepatic biliary drainage, VFPP virtual fluoroscopic preprocedural planning

* A significant difference

It was necessary to change the targeted bile duct in two patients in the coronal CT group and in one patient in the VFPP group because we failed to puncture the bile duct. There were no statistically significant differences between the groups.

There were also no significant differences in the targeted bile duct, diameter and depth of target bile, breath-holding, number of puncture attempts, change in the targeted bile duct, and exchange of the drainage catheter. The X-ray fluoroscopy time and the procedure time were significantly shorter in the VFPP group than in the coronal CT group (196 vs. 334 s, $P < 0.05$; and 16.0 vs. 27.2 min, $P < 0.05$).

There were six procedure-related minor complications [Society of Interventional Radiology (SIR) Classification

B]. One patient in each group developed mild pain at the puncture site, and two patients in each group developed mild abdominal pain. One procedure-related major complication (SIR Classification D) occurred. One patient in the coronal CT group experienced subcapsular hepatic hematoma, but this patient was successfully treated conservatively.

Discussion

The importance of using imaging in preprocedural planning for patients with bile duct obstruction cannot be overemphasized because the level of obstruction and bile

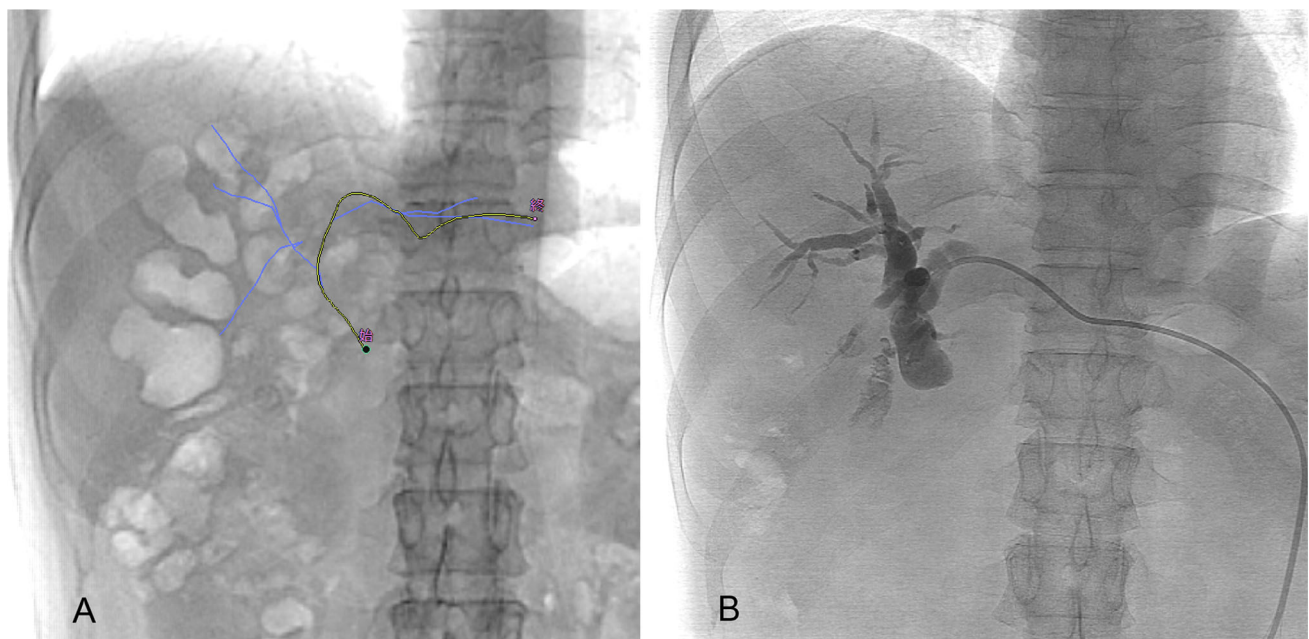


Fig. 2 An 85-year-old female with obstructive jaundice due to pancreatic cancer. **A** We used this VFPP image as the reference image. The yellow line shows the course of B3 to the common bile duct. The annotation is the obstruction in the common bile duct. The

blue lines show neighboring bile ducts. The VFPP image is similar to the fluoroscopy image. **B** The fluoroscopy image was obtained by infusing a small amount of dilute contrast media through the catheter VFPP

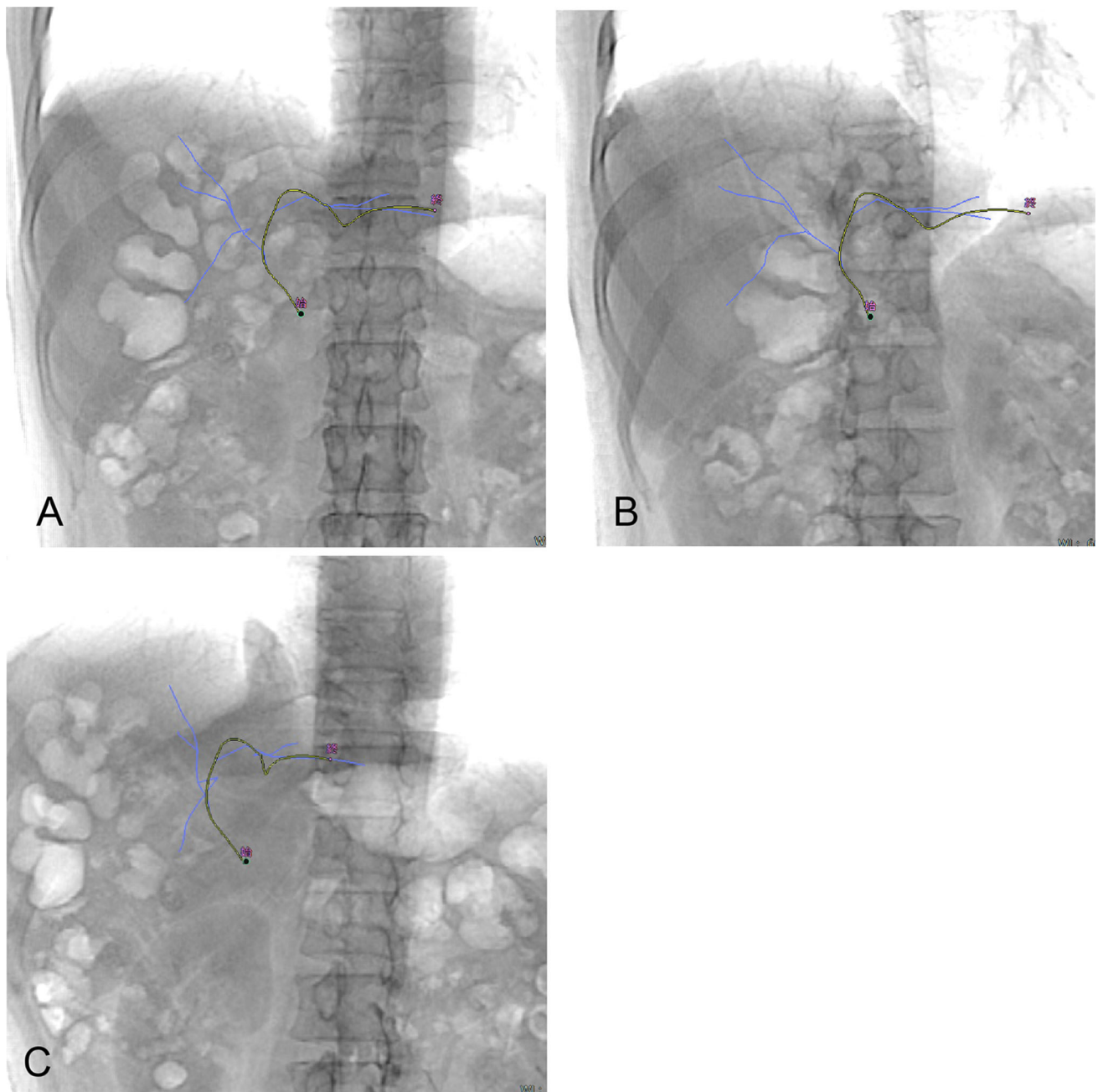


Fig. 3 The VFPP makes it possible to display the three-dimensional virtual fluoroscopic image at any angle. **A** The frontal view of B3 to the common bile duct. **B** The right anterior view (RAO) 25° of B3 to

the common bile duct. **C** The left anterior view (LAO) 25° of B3 to the common bile duct VFPP

duct anatomy are most easily determined by MDCT or by magnetic resonance cholangiopancreatography [7]. However, it is impossible by MDCT to display the bile duct anatomy and obstruction in one image. Magnetic resonance cholangiopancreatography displays the bile duct anatomy and obstruction in one image, but the image is not similar to a fluoroscopy image. By contrast, a VFPP image displays the bile duct anatomy and obstruction in only one image that is similar to a fluoroscopy image (Fig. 2).

Because the lines can be displayed at any angle in the 3-dimensional virtual fluoroscopic image, we could also choose an appropriate working angle beforehand and perform the procedure in this state (Fig. 3). Moreover, VFPP images are effective in the situation of a targeted bile duct with a bending and meandering course.

Using intraoperative referencing VFPP images enables a physician to advance the guidewire precisely and quickly into the common bile duct under X-ray fluoroscopy

guidance. Therefore, it was possible to shorten the X-ray fluoroscopy time and procedure time by using VFPP. Shortening the X-ray fluoroscopy time may contribute to lower amounts of radiation exposure to the patient and staff.

One-half of early complications are procedure-related [8–10]. These complications include pain at the puncture site, bile leak with the risk of biliary peritonitis and biloma formation, cholangitis, septicemia, and bleeding [9, 10]. Adequate preprocedural planning may help to reduce these complications.

New navigation systems are used in various procedures. The feasibility of automated tumor-feeders detection software for hepatocellular carcinoma and fluoroscopy with magnetic resonance angiography/computerized tomographic angiography fusion guidance for peripheral artery interventions have been reported in the literature [12–14]. These navigation systems are quite useful, but they are not available at all medical institutions. By contrast, VFPP is easy to prepare if only the volume data from MDCT and a workstation are available [11]. The introduction of a new device is therefore unnecessary, and an extra financial burden is avoided.

In this study, we were able to create VFPP from contrast-enhanced MDCT in all patients, except for one patient. All bile ducts were dilated. However, VFPP may take a long time if only plain MDCT images are available or if the bile duct does not dilate.

In this study, the X-ray fluoroscopy time was 73–783 s (mean time 271 s). Kloeckner et al. [15] reported that the mean X-ray fluoroscopy times of right- and left-sided PTBD were 13.5 and 16.6 min. The mean PTBD time was longer in that study than in our study. There are two reasons for this finding. First, we performed PTBD in a one-step method using an 18-gauge needle instead of in the two-step method because all patients in this study had dilated ducts [10]. Second, in only two patients, we placed the internal–external catheter beyond the obstruction of the common hepatic duct, and we placed the obligatory external drainage catheter above the obstruction in many patients.

This study had several limitations. First, it was a single-center study. Second, the retrospective nature of the study may also limit the conclusions drawn from it. Third, the number of patients in the VFPP group and CT group was uneven, which may have introduced bias in the results. However, the baseline characteristics of patients in both groups were equivalent. Fourth, the accuracy of VFPP depends on the planner because the lines in VFPP are drawn manually. However, all VFPP procedures were performed by two authors and included a radiologist and radiological technician. It was believed that the VFPP images were sufficient to be used as reference images.

Conclusion

Intraoperative referencing of the VFPP image during PTBD can intuitively be a useful tool for better localization of the guidewire in the bile duct. This procedure thereby shortens the X-ray fluoroscopy time and procedure time while minimizing radiation exposure and complications.

Compliance with Ethical Standards

Conflict of interest The authors have no conflicts of interest to declare.

References

1. Takada T, Hanyu F, Kobayashi S, Uchida Y. Percutaneous transhepatic cholangial drainage: direct approach under fluoroscopic control. *J Surg Oncol.* 1976;8:83–97.
2. Makuuchi M, Bandai Y, Ito T, Watanabe G, Wada T, Abe H, Muroi T. Ultrasonically percutaneous transhepatic bile drainage: a single-step procedure without cholangiography. *Radiology.* 1980;136:165–9.
3. Baxter-Smith DC, Temple JG, Howarth F. Palliative percutaneous transhepatic drainage for inoperable obstructive jaundice. *Ann R Coll Surg Engl.* 1982;64:394–6.
4. Nagino M, Hayakawa N, Nimura Y, Dohke M, Kitagawa S. Percutaneous transhepatic biliary drainage in patients with malignant biliary obstruction of the hepatic confluence. *Hepato-gastroenterology.* 1992;39:296–300.
5. Saad WE, Wallace MJ, Wojak JC, Kundu S, Cardella JF. Quality improvement guidelines for percutaneous transhepatic cholangiography, biliary drainage, and percutaneous cholecystostomy. *J Vasc Interv Radiol.* 2010;21:789–95.
6. Hamlin J, Friedman M, Stein M, Bray J. Percutaneous biliary drainage: complications of 118 consecutive catheterizations. *Radiology.* 1986;158:199–202.
7. Covey AM, Brown KT. Percutaneous transhepatic biliary drainage. *Tech Vasc Interv Radiol.* 2008;11:14–20.
8. Saluja SS, Gulati M, Garg PK, Pal H, Pal S, Sahni P, Chat-topadhyay TK. Endoscopic or percutaneous biliary drainage for gallbladder cancer: a randomized trial and quality of life assessment. *Clin Gastroenterol Hepatol.* 2008;6:944–50.
9. Walter T, Ho CS, Horgan AM, Warkentin A, Gallinger S, Greig PD, Kortan P, Knox JJ. Endoscopic or percutaneous biliary drainage for Klatskin tumors? *J Vasc Interv Radiol.* 2013;24:113–21.
10. Madhusudhan KS, Gamanagatti S, Srivastava DN, Gupta AK. Radiological interventions in malignant biliary obstruction. *World J Radiol.* 2016;8:518–29.
11. Fukusumi M, Ichinose Y, Arimoto Y, Takeoka S, Homma C, Matsuoka H, Mouri A, Hamamoto Y, Matsumoto J, Kamimura M. Bronchoscopy for pulmonary peripheral lesions with virtual fluoroscopic preprocedural planning combined with EBUS-GS: a pilot study. *J Bronchol Interv Pulmonol.* 2016;23:92–7.
12. Miyayama S, Yamashiro M, Hashimoto M, Hashimoto N, Ikuno M, Okumura K, Yoshida M, Matsui O. Identification of small hepatocellular carcinoma and tumor-feeding branches with cone-beam CT guidance technology during transcatheter arterial chemoembolization. *J Vasc Interv Radiol.* 2013;24:501–8.
13. Miyayama S, Yamashiro M, Ikuno M, Okumura K, Yoshida M. Ultrasensitive transcatheter arterial chemoembolization for small hepatocellular carcinoma guided by automated tumor-feeders

- detection software: technical success and short-term tumor response. *Abdom Imaging*. 2014;39:645–56.
14. Sailer AM, de Haan MW, de Graaf R, van Zwam WH, Schurink GWH, Nelemans PJ, Wildberger JE, Das M. Fusion guidance in endovascular peripheral artery interventions: a feasibility study. *Cardiovasc Interv Radiol*. 2015;38:314–21.
 15. Kloeckner R, Bersch A, Dos Santos DP, Schneider J, Düber C, Pitton MB. Radiation exposure in nonvascular fluoroscopy-guided interventional procedures. *Cardiovasc Interv Radiol*. 2012;35:613–20.